High-power noise-like pulse generation using a 1.56-μm all-fiber laser system

Shih-Shian Lin,[1] Sheng-Kwang Hwang,[2,3] and Jia-Ming Liu[1,4,*]

[1]*Institute of Photonic System, National Chiao Tung University, Tainan, Taiwan*
[2]*Department of Photonics, National Cheng Kung University, Tainan, Taiwan*
[3]*Advanced Optoelectronic Technology Center, National Cheng Kung University, Tainan, Taiwan*
[4]*Electrical Engineering Department, University of California, Los Angeles, California, USA*
[*]*liu@seas.ucla.edu*

Abstract: We demonstrated an all-fiber, high-power noise-like pulse laser system at the 1.56-μm wavelength. A low-power noise-like pulse train generated by a ring oscillator was amplified using a two-stage amplifier, where the performance of the second-stage amplifier determined the final output power level. The optical intensity in the second-stage amplifier was managed well to avoid not only the excessive spectral broadening induced by nonlinearities but also any damage to the device. On the other hand, the power conversion efficiency of the amplifier was optimized through proper control of its pump wavelength. The pump wavelength determines the pump absorption and therefore the power conversion efficiency of the gain fiber. Through this approach, the average power of the noise-like pulse train was amplified considerably to an output of 13.1 W, resulting in a power conversion efficiency of 36.1% and a pulse energy of 0.85 μJ. To the best of our knowledge, these amplified pulses have the highest average power and pulse energy for noise-like pulses in the 1.56-μm wavelength region. As a result, the net gain in the cascaded amplifier reached 30 dB. With peak and pedestal widths of 168 fs and 61.3 ps, respectively, for the amplified pulses, the pedestal-to-peak intensity ratio of the autocorrelation trace remains at the value of 0.5 required for truly noise-like pulses.

OCIS codes: (140.3280) Laser amplifiers; (060.2320) Fiber optics amplifiers and oscillators; (140.5560) Pumping; (140.4480) Optical amplifiers; (120.4640) Optical instruments; (120.4820) Optical systems.

References and links

1. M. Horowitz, Y. Barad, and Y. Silberberg, "Noiselike pulses with a broadband spectrum generated from an erbium-doped fiber laser," Opt. Lett. **22**(11), 799–801 (1997).
2. D. Tang, L. Zhao, and B. Zhao, "Soliton collapse and bunched noise-like pulse generation in a passively mode-locked fiber ring laser," Opt. Express **13**(7), 2289–2294 (2005).
3. L. M. Zhao, D. Y. Tang, T. H. Cheng, H. Y. Tam, and C. Lu, "120 nm bandwidth noise-like pulse generation in an erbium-doped fiber laser," Opt. Commun. **281**(1), 157–161 (2008).
4. S. Kobtsev, S. Kukarin, S. Smirnov, S. Turitsyn, and A. Latkin, "Generation of double-scale femto/pico-second optical lumps in mode-locked fiber lasers," Opt. Express **17**(23), 20707–20713 (2009).
5. O. Pottiez, R. Grajales-Coutiño, B. Ibarra-Escamilla, E. A. Kuzin, and J. C. Hernández-García, "Adjustable noiselike pulses from a figure-eight fiber laser," Appl. Opt. **50**(25), E24–E31 (2011).
6. L. A. Vazquez-Zuniga and Y. Jeong, "Super-broadband noise-like pulse erbium-doped fiber ring laser with a highly nonlinear fiber for Raman gain enhancement," IEEE Photon. Technol. Lett. **24**(17), 1549–1551 (2012).
7. A. Boucon, B. Barviau, J. Fatome, C. Finot, T. Sylvestre, M. W. Lee, P. Grelu, and G. Millot, "Noise-like pulses generated at high harmonics in a partially-mode-locked km-long Raman fiber laser," Appl. Phys. B **106**(2), 283–287 (2012).
8. S. Smirnov, S. Kobtsev, S. Kukarin, and A. Ivanenko, "Three key regimes of single pulse generation per round trip of all-normal-dispersion fiber lasers mode-locked with nonlinear polarization rotation," Opt. Express **20**(24), 27447–27453 (2012).
9. M. Suzuki, R. A. Ganeev, S. Yoneya, and H. Kuroda, "Generation of broadband noise-like pulse from Yb-doped fiber laser ring cavity," Opt. Lett. **40**(5), 804–807 (2015).
10. V. Goloborodko, S. Keren, A. Rosenthal, B. Levit, and M. Horowitz, "Measuring temperature profiles in high-power optical fiber components," Appl. Opt. **42**(13), 2284–2288 (2003).

#239720 Received 24 Apr 2015; revised 13 Jun 2015; accepted 15 Jun 2015; published 6 Jul 2015

11. S. Keren and M. Horowitz, "Interrogation of fiber gratings by use of low-coherence spectral interferometry of noiselike pulses," Opt. Lett. **26**(6), 328–330 (2001).
12. S. Keren, E. Brand, Y. Levi, B. Levit, and M. Horowitz, "Data storage in optical fibers and reconstruction by use of low-coherence spectral interferometry," Opt. Lett. **27**(2), 125–127 (2002).
13. S. Keren, A. Rosenthal, and M. Horowitz, "Measuring the structure of highly reflecting fiber Bragg gratings," IEEE Photon. Technol. Lett. **15**(4), 575–577 (2003).
14. Y. Takushima, K. Yasunaka, Y. Ozeki, and K. Kikuchi, "87 nm bandwidth noise-like pulse generation from erbium-doped fibre laser," Electron. Lett. **41**(7), 399–400 (2005).
15. J. C. Hernandez-Garcia, O. Pottiez, and J. M. Estudillo-Ayala, "Supercontinuum generation in a standard fiber pumped by noise-like pulses from a figure-eight fiber laser," Laser Phys. **22**(1), 221–226 (2012).
16. A. Zaytsev, C. H. Lin, Y. J. You, C. C. Chung, C. L. Wang, and C. L. Pan, "Supercontinuum generation by noise-like pulses transmitted through normally dispersive standard single-mode fibers," Opt. Express **21**(13), 16056–16062 (2013).
17. J. C. Hernandez-Garcia, O. Pottiez, J. M. Estudillo-Ayala, and R. Rojas-Laguna, "Numerical analysis of a broadband spectrum generated in a standard fiber by noise-like pulses from a passively mode-locked fiber laser," Opt. Commun. **285**(7), 1915–1919 (2012).
18. S. S. Lin, S. K. Hwang, and J. M. Liu, "Supercontinuum generation in highly nonlinear fibers using amplified noise-like optical pulses," Opt. Express **22**(4), 4152–4160 (2014).
19. X. W. Zheng, Z. C. Luo, H. Liu, N. Zhao, Q. Y. Ning, M. Liu, X. H. Feng, X. B. Xing, A. P. Luo, and W. C. Xu, "High-energy noiselike rectangular pulse in a passively mode-locked figure-eight fiber laser," Appl. Phys. Express **7**(4), 042701 (2014).
20. P. Polynkin, A. Polynkin, D. Panasenko, N. Peyghambarian, M. Mansuripur, and J. Moloney, "All-fiber passively mode-locked laser oscillator at 1.5 μm with watts-level average output power and high repetition rate," Opt. Lett. **31**(5), 592–594 (2006).
21. A. K. Zaytsev, C. H. Lin, Y. J. You, F. H. Tsai, C. L. Wang, and C. L. Pan, "A controllable noise-like operation regime in a Yb-doped dispersion-mapped fiber ring laser," Laser Phys. Lett. **10**(4), 045104 (2013).
22. H. L. Yu, P. F. Ma, R. M. Tao, X. L. Wang, P. Zhou, and J. B. Chen, "High average/peak power linearly polarized all-fiber picosecond MOPA seeded by mode-locked noise-like pulses," Laser Phys. Lett. **12**(6), 065103 (2015).
23. O. Lumholt, T. Rasmussen, and A. Bjarklev, "Modelling of extremely high concentration erbium-doped silica waveguides," Electron. Lett. **29**(5), 495–496 (1993).
24. Q. Wang and N. K. Dutta, "Er-Yb double-clad fiber amplifier," Opt. Eng. **43**(5), 1030–1034 (2004).
25. J. Nilsson, P. Scheer, and B. Jaskorzynska, "Modeling and optimization of short Yb^{3+}-sensitized Er^{3+}-doped fiber amplifiers," IEEE Photon. Technol. Lett. **6**(3), 383–385 (1994).
26. C. Strohhöfer and A. Polman, "Relationship between gain and Yb^{3+} concentration in Er^{3+}–Yb^{3+} doped waveguide amplifiers," J. Appl. Phys. **90**(9), 4314–4320 (2001).
27. C. Lester, A. Bjarklev, T. Rasmussen, and P. G. Dinesen, "Modeling of Yb^{3+}-sensitized Er^{3+}-doped silica waveguide amplifiers," J. Lightwave Technol. **13**(5), 740–743 (1995).
28. M. Achtenhagen, R. J. Beeson, F. Pan, B. Nyman, and A. Hardy, "Gain and noise in ytterbium-sensitized erbium-doped fiber amplifiers: measurements and simulations," J. Lightwave Technol. **19**(10), 1521–1526 (2001).
29. B. L. Volodin, S. V. Dolgy, E. D. Melnik, E. Downs, J. Shaw, and V. S. Ban, "Wavelength stabilization and spectrum narrowing of high-power multimode laser diodes and arrays by use of volume Bragg gratings," Opt. Lett. **29**(16), 1891–1893 (2004).
30. M. Fukuda, T. Mishima, N. Nakayama, and T. Masuda, "Temperature and current coefficients of lasing wavelength in tunable diode laser spectroscopy," Appl. Phys. B **100**(2), 377–382 (2010).
31. A. F. J. Runge, C. Aguergaray, N. G. R. Broderick, and M. Erkintalo, "Coherence and shot-to-shot spectral fluctuations in noise-like ultrafast fiber lasers," Opt. Lett. **38**(21), 4327–4330 (2013).
32. P. Maine, D. Strickland, P. Bado, M. Pessot, and G. Mourou, "Generation of ultrahigh peak power pulses by chirped pulse amplification," IEEE J. Quantum Electron. **24**(2), 398–403 (1988).

1. Introduction

Noise-like pulses generated by fiber lasers have been proposed for the generation of structureless, broad spectra covering tens or hundreds of nanometers [1–9]. Such pulses are composed of picosecond wavepackets with a fine inner structure of femtosecond pulses that have stochastically varying widths and peak intensities. This temporal feature leads to a double-scaled autocorrelation trace that has a femtosecond peak riding upon a wide and smooth picosecond pedestal, suggesting a characteristic of low temporal coherence. Noise-like pulses find various applications that take advantage of their low temporal coherence, such as optical metrology, optical sensing [10], optical coherence tomography, and optical communications [11–13]. By taking advantage of their smooth and broad spectra, noise-like pulses have also been used as pump pulses for supercontinuum generation in nonlinear fibers [14–18]. For many of these applications, a high optical power is beneficial and therefore preferred. One approach to increasing the optical power is to adopt different gain media and

#239720 Received 24 Apr 2015; revised 13 Jun 2015; accepted 15 Jun 2015; published 6 Jul 2015

laser structures for the laser oscillators. For example, in the 1.56-μm wavelength region, while noise-like pulses with a pulse energy of 135 nJ and an average power of 0.04 W were generated by using an erbium-doped fiber laser [19], noise-like pulses with a pulse energy of 25 nJ and an average power of 2.4 W were demonstrated by adopting an erbium/ytterbium-codoped fiber laser [20]; in the 1.06-μm wavelength region, a noise-like pulse train with a pulse energy of 47 nJ and an average power of 1.45 W was achieved in an ytterbium-doped fiber laser [21]. As noted, however, the output power of a fiber laser is somehow limited from the viewpoint of practical application. Using optical fiber amplifiers, on the other hand, to substantially boost up the optical power of noise-like pulses should be an effective and efficient approach, but this approach has not received much attention. Typically, ytterbium-doped fibers are used as the gain medium for optical power amplification in the 1.06-μm wavelength region, whereas erbium-doped fibers are used in the 1.56-μm wavelength region. In general, the power conversion efficiency of the former is inherently much higher than that of the latter, making the conditions and challenges different for power amplification between the two wavelength regions. Therefore, even though a pulse energy of 22.6 μJ and an average power of 423 W were very recently achieved by a three-stage ytterbium-doped fiber amplifier for noise-like pulses at 1.06 μm [22], there has not been any investigation reported yet for noise-like pulses at 1.56 μm with an average power of 10 W and beyond. In this work, we report on the development of an all-fiber laser system consisting of fiber amplifiers for high-power noise-like pulse generation at 1.56 μm.

Erbium-doped silica fibers are a popular gain medium for 1.56-μm fiber amplifiers. A high erbium concentration in a gain fiber, however, causes clusters formed by neighboring erbium ions, which result in a quenching process that reduces the power conversion efficiency of a fiber amplifier [23–25]. Codoping with ytterbium in an erbium-doped fiber promotes power scaling above the watt level and allows a significant increase in pump absorption. To further improve the power conversion efficiency of erbium/ytterbium-codoped fiber amplifiers, studies focusing on the concentration ratio of erbium and ytterbium ions [25–27], the length of the gain fiber [28], and the pumping schemes were conducted. For a given fiber amplifier, however, these factors are already determined and therefore are difficult, if not impossible, to adjust during operation by varying externally controllable operating conditions for the maximization of the power conversion efficiency. Fiber amplifiers are normally pumped by high-power diode lasers that are each driven by a large drive current. Consequently, the output wavelength of a high-power pump diode laser shifts significantly with its drive current due to heating of the diode by the large current [29, 30]. The pump absorption of the gain fiber changes in response to this variation in the pump wavelength. This absorption change strongly influences the power conversion efficiency of a fiber amplifier, especially one pumped at a wavelength close to its peak absorption wavelength. Proper control of the pump wavelength should therefore serve as a simple and flexible way to improve and optimize the power conversion efficiency of a given fiber amplifier.

Hence, in this work, we report on the development of an all-fiber oscillator-amplifier system producing high-power noise-like pulses. During the pulse amplification at different power levels, the spectral broadening induced by nonlinearities was well controlled to avoid gain suppression and device damage in the amplifiers. Moreover, to enhance the optical power of noise-like pulses to the highest possible level, we particularly focused on the investigation of how the power conversion efficiency of a given erbium/ytterbium-codoped fiber amplifier can be maximized by properly adjusting the wavelength of the pump diode laser under different system operating conditions. The pump diode laser has a common wavelength-stabilized design, available from the mature low-cost diode laser technology. Thus, the output wavelength can be stabilized and tuned over a large range by controlling the diode temperature although it drifts with the drive current. By applying this approach of pump-wavelength adjustment to the amplification of a noise-like pulse train, we were able to considerably increase average output power of the pulse train to 13.1 W with a pulse energy of 0.85 μJ at a pump power of 35.7 W, achieving a power conversion efficiency of 36.1%, without affecting the pulse characteristics through amplification.

#239720 Received 24 Apr 2015; revised 13 Jun 2015; accepted 15 Jun 2015; published 6 Jul 2015

2. Experimental setup

Figure 1(a) shows the schematic of the all-fiber laser system under study, which consisted of a seed laser generating noise-like pulses and a two-stage fiber amplifier boosting the optical power of the pulses. The seed laser was a fiber ring laser that had a cavity length of about 12.7 m, as shown in Fig. 1(b). The ring cavity contained a 0.6-m erbium-doped fiber (Liekki ER80-8/125) that had a peak absorption coefficient of 80 dB/m at 1530 nm. A 980 nm/1550nm wavelength division multiplexing coupler was used to launch the pump at a power level of 480 mW from a 976-nm laser diode (JDSU S30-7602-660). A polarization-dependent isolator between two in-line polarization controllers was used to ensure unidirectional operation and polarization selection. Together with the two polarization controllers, a nonlinear switching mechanism was achieved through nonlinear polarization rotation, which led to the generation of noise-like pulses. A coupler was utilized as the output port of the ring cavity to extract 10% of the laser power. The average output power of the fiber laser was 13 mW, which was guided into the fiber amplifiers.

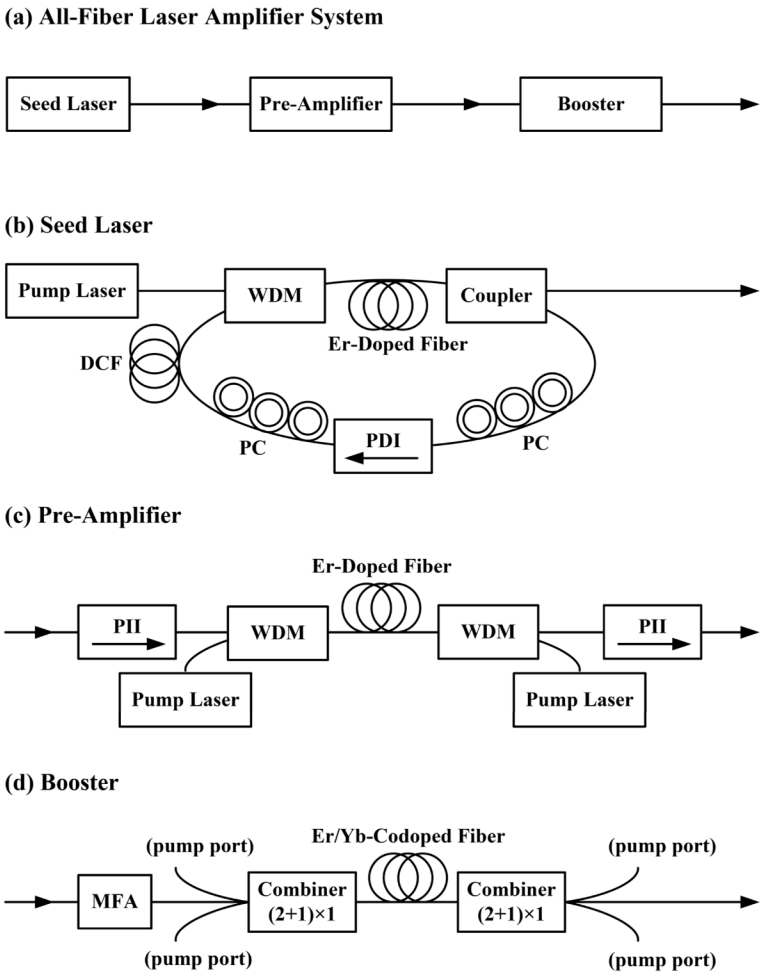

Fig. 1. Schematics of (a) the all-fiber laser amplifier system, (b) the seed laser, (c) the pre-amplifier, and (d) the booster. WDM, wavelength division multiplexer; PC, polarization controller; PDI, polarization-dependent isolator; DCF, dispersion compensation fiber; PII: Polarization-independent isolator; MFA: mode-field adaptor.

#239720 Received 24 Apr 2015; revised 13 Jun 2015; accepted 15 Jun 2015; published 6 Jul 2015

Two cascaded fiber amplifiers, a first-stage pre-amplifier based on an erbium-doped fiber and a second-stage booster based on an erbium/ytterbium-codoped fiber, were used to promote the signal power. As shown in Fig. 1(c), an erbium-doped fiber (Liekki ER80-8/125) of 1.2 m length was used as the gain medium for the pre-amplifier. Two 976-nm laser diodes (JDSU S30-7602-660 and S30-7602-600) were used to bi-directionally pump the pre-amplifier. Two polarization-independent isolators were separately placed at the input and the output ports of the pre-amplifier to eliminate optical reflection back to the seed laser and from the booster, respectively. The booster, as shown in Fig. 1(d), was composed of a mode-field adaptor, two signal–pump power combiners, and a 2.5-m erbium/ytterbium-codoped double-clad fiber (Nufern LMA-EYDF-25P/300-HE). A mode-field adaptor was employed to match the two different fiber core diameters of the cascaded amplifiers. Note that an 8-μm standard single-mode fiber and a 25-μm large-mode-area fiber were used in the pre-amplifier and the booster, respectively. A convenient way to scale up the power level of a rare-earth-doped fiber amplifier is to use a double-clad gain fiber, in which the signal and pump power respectively propagate in the core and the inner cladding, to alter the power capacity. Each end of the double-clad gain fiber was connected with a signal–pump power combiner, which included two fiber pigtails for coupling the pump power into the inner cladding layer of the gain fiber. High-power fiber-coupled diode lasers (Oclaro BMU25A-975-01-R03) were used as the pumping sources with heat sinks to stabilize and adjust their emission wavelengths. Because the pump lasers were commercially packaged units, the temperature being monitored was that on the case of a unit rather than that at the junction of the diode. At the system output, an anti-reflection-coated lens with a focal length of 5 cm collimated the laser beam. The amplified signal beam separated from the laser beam by a long-pass filter was monitored.

An optical spectrum analyzer (Anritsu MS9740A) was used to analyze the spectral features of the noise-like pulses at the outputs of the fiber ring laser, the pre-amplifier, and the booster. The pulse train was recorded with a 1.5-GHz photodiode (Electro-Optics Technology ET-3010) and displayed on a 350-MHz real-time oscilloscope (Keysight DSO-X 3034A). A background-free intensity autocorrelator (Femtochrome FR-103XL) was used to study the autocorrelation traces of the noise-like pulses.

3. Results and analysis

3.1 Generation of noise-like pules

A noise-like pulse train of a 15.5 MHz repetition rate was generated from the seed laser, as shown in Fig. 2(a). The average power of the seed noise-like pulses was 13 mW, corresponding to a pulse energy of 0.8 nJ. The optical spectrum, shown in Fig. 2(b), had a central wavelength of 1.56 μm and a 3-dB spectral width of 13 nm. In the noise-like pulse train, the spectral components of the optical fields are highly uncorrelated [31]. Each single-shot optical spectrum of the pulses is highly structured [31]. The ensemble average of the shot-to-shot spectra brought on a smooth optical spectrum, which was recorded using a conventional spectrum analyzer. Figures 2(c) and 2(d) show in two different scales the autocorrelation trace of these optical pulses. The autocorrelation trace of the noise-like pulses showed a narrow coherent peak of 383 fs width on a wide pedestal of 51.8 ps width, and the intensity ratio of the pedestal to the peak was about 0.5. The pulse profile was consistent with the inherent characteristics of the noise-like pulses of a fiber laser. Note that the widths of the peak and the pedestal were defined as the full widths at half-maximum of their Gaussian fitting curves. The wide and smooth pedestal indicates that the optical fields under investigation were composed of picosecond wavepackets with fine inner structures of

#239720 Received 24 Apr 2015; revised 13 Jun 2015; accepted 15 Jun 2015; published 6 Jul 2015

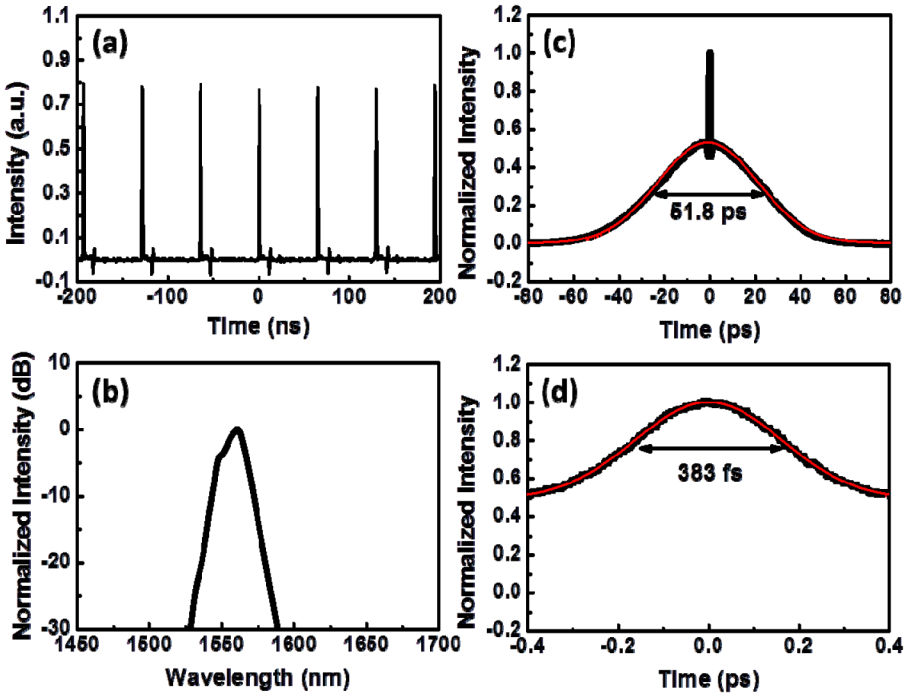

Fig. 2. (a) Output pulse train, (b) optical spectrum, (c) autocorrelation trace, and (d) magnified autocorrelation trace of the noise-like pulses from the seed laser. Red curves in (c) and (d) are the Gaussian fittings of the pedestal and the peak, respectively.

randomly varying noisy pulses; the narrow peak suggests that the noisy pulses within the wavepackets had femtosecond temporal widths. Moreover, the pedestal-to-peak intensity ratio of 0.5 indicates that the intensities of the femtosecond pulses varied stochastically [1, 4, 7]. Such random intensity fluctuations of the noisy femtosecond pulses led to the intensity fluctuations of the wavepackets seen in the pulse train, as presented in Fig. 2(a). The observed characteristics of the autocorrelation trace together with the broad and smooth optical spectrum were identifying features common to the noise-like pulses reported in the literature [1–8].

3.2 Amplification of noise-like pulses with pre-amplifier

The average power of the noise-like pulse train at the output of the preamplifier, which was obtained from amplifying the seed pulse train, increased linearly with the pump power of the pre-amplifier. The maximum output power of 0.21 W was obtained at a pump power level of 0.96 W, corresponding to a power conversion efficiency of 21%. This also means that the pulse energy increased from 0.8 to 13.5 nJ. The 3-dB spectral width of the amplified noise-like pulses broadened significantly from 13 to 21 nm, as shown in Fig. 3(a). It was clear that the noise-like pulses experienced some nonlinear optical effects, such as self-phase modulation, during the pre-amplification process. Note that, in regular-pulse amplification, the pulse width is always stretched out in time through using extra dispersive media prior to amplification [32]. This technique decreases the peak power of the pulse to avoid inducing excessive nonlinear effects in the amplifier. Such temporal stretching was not conducted in this study because it was not effective and not necessary for the noise-like pulses at the power level of our pre-amplifier [8]. The temporal features of the pre-amplified noise-like pulses are presented in Figs. 3(b) and 3(c). The peak width of the autocorrelation trace decreased significantly from the 383 fs width of the seed laser pulses to 207 fs, indicating that the temporal coherence of the pre-amplified noise-like pulses was reduced. Meanwhile, the

#239720 Received 24 Apr 2015; revised 13 Jun 2015; accepted 15 Jun 2015; published 6 Jul 2015

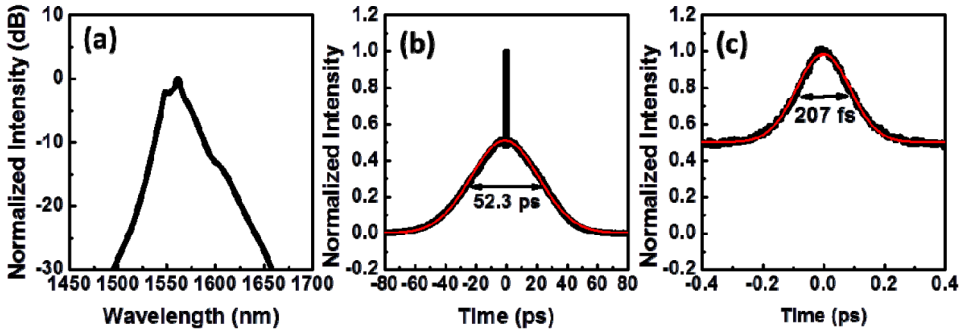

Fig. 3. (a) Output optical spectrum, (b) autocorrelation trace, and (c) magnified autocorrelation trace of noise-like pulses from the output of the pre-amplifier. Red curves in (b) and (c) are the Gaussian fittings of the pedestal and the peak, respectively.

pedestal width increased only slightly from 51.8 ps to 52.3 ps, indicating that the wavepackets slightly expanded. A similar double-scaled autocorrelation trace was observed with a pedestal-to-peak intensity ratio of 0.5, confirming a noise-like characteristic after pre-amplification.

3.3 Amplification of continuous-wave optical fields with booster

To further increase the optical power of the noise-like pulses, a booster following the pre-amplifier was used. As will be demonstrated in the following analyses, the optical power does not necessarily increase linearly with the pump power of the booster as in the case of the pre-amplifier. Therefore, before sending the noise-like pulses into the booster, an investigation on the conditions and the resulting characteristics of amplification by the booster were first conducted by sending continuous-wave optical fields through the booster to gain a clear understanding of the system behavior and also to serve as an operating guidance for pulse amplification. For this purpose, a fiber-coupled distributed-feedback diode laser (Fujitsu FLD5F6CX-J34) emitting continuous-wave optical fields at a wavelength of 1550 nm with an output power of 8 mW was used. Its power was first amplified to 0.21 W by the pre-amplifier pumped at a pump power level of 1.01 W before it was sent into the booster.

3.3.1 Characteristics of pump laser and gain fiber

The key parameters that influenced the output power and conversion efficiency of the booster are the power and wavelength of the pump laser and the pumping scheme. The power and wavelength of the pump laser are determined by both its drive current and its temperature. Therefore, in our experiment, we controlled and monitored the drive current and the temperature of the pump laser to adjust the pump power and pump wavelength. The drive current and the temperature could be separately varied and stabilized, as shown in Fig. 4(a). At a fixed temperature, the wavelength of the pump laser was found to be a linear function of the drive current with a wavelength–current coefficient of 1.0 nm/A for drive currents ranging from 1 to 10 A. At a fixed derive current within this range, the wavelength of the pump laser linearly increased with temperature at a rate of 0.3 nm/°C within the range of temperatures from 20 to 50 °C. Therefore, the range of wavelength variation influenced by either the drive current or the temperature was 9 nm when one of the two parameters was fixed, but the whole range of variation was 18 nm when both parameters were varied. The output power of the pump laser was measured for different drive currents and temperatures, as also plotted in Fig. 4(a).

The drift of the pump wavelength with the drive current and the temperature influenced the effective pump absorption of the gain fiber, as demonstrated in Fig. 4(b) where the pump absorption coefficient of the gain fiber as a function of the pump wavelength is shown. To facilitate the following discussion, the pump absorption coefficient is also presented in

#239720 Received 24 Apr 2015; revised 13 Jun 2015; accepted 15 Jun 2015; published 6 Jul 2015

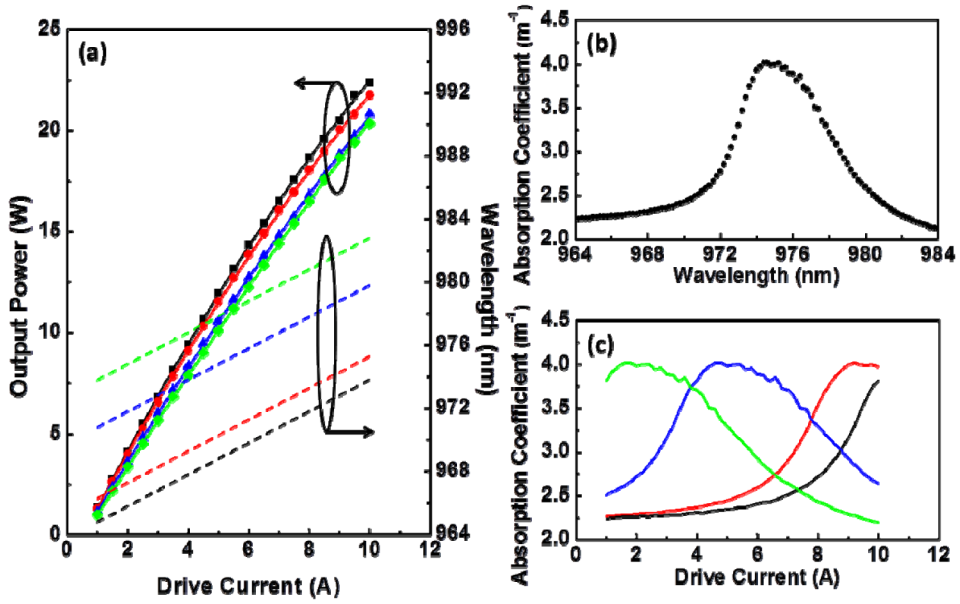

Fig. 4. (a) Output power (solid curves) and output wavelength (dash curves) of the pump diode laser versus its drive current at different temperatures. (b) Absorption coefficient of the gain fiber versus the pump wavelength. (c) Absorption coefficient of the gain fiber versus the drive current of pump diode laser at different temperatures. The black, red, blue, and green curves represent temperatures of 20 °C, 25 °C, 40 °C, and 50 °C, respectively.

Figure 4(c) as a function of the drive current of the pump laser at different temperatures according to the relation between Figs. 4(a) and 4(b). The effective pump absorption could therefore be well controlled by adjusting the drive current and temperature of the pump laser. For instance, the pump absorption coefficient increased by approximately 73% (from 2.2 to 3.8 m^{-1}) when the drive current was increased from 1 A to 10 A at a constant temperature of 20 °C, as shown in Fig. 4(c). By contrast, it dropped by approximately 42% (from 3.8 to 2.2 m^{-1}) when the drive current was increased from 1 A to 10 A at a constant temperature of 50 °C. Hence, it is clear that the temperature of the pump laser has to be carefully chosen and monitored for each drive current level to maximize the power conversion efficiency of the booster.

3.3.2 Power conversion efficiency vs. pump wavelength

To maximize the power conversion efficiency as suggested above, it is necessary to understand how the output signal power of the booster varies with the pump power by operating the pump laser at a fixed temperature while its emission wavelength varies with the drive current, as shown in Fig. 5(a), and how it varies with the pump power by operating the pump laser at a fixed emission wavelength while its temperature varies with the drive current, as shown in Fig. 5(b). At different operating temperatures, different drive currents were required for the pump laser to deliver the same pump power, as indicated in Fig. 4(a). To facilitate the following discussion with the information of the drive current also shown in Fig. 5, a nominal drive current was used instead for each pump power at all temperatures, which was obtained by averaging different drive currents required for different temperatures under study to achieve a specific pump power. To determine the best power conversion efficiency under study, the forward and backward pumping schemes were separately implemented by using the same pump laser for different operating conditions.

#239720 Received 24 Apr 2015; revised 13 Jun 2015; accepted 15 Jun 2015; published 6 Jul 2015

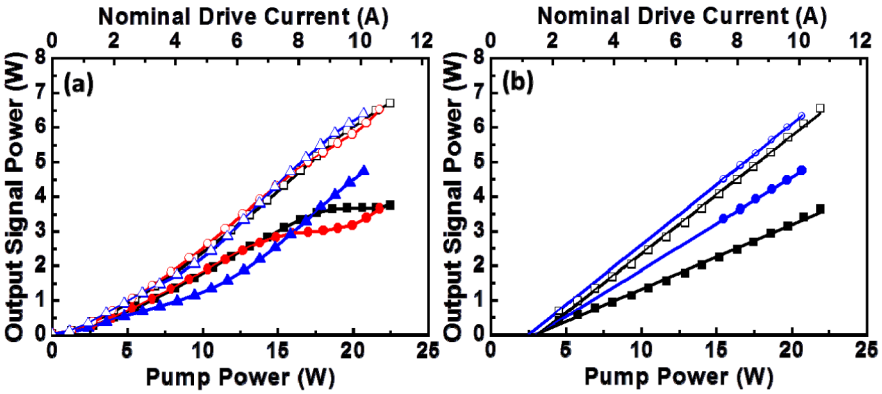

Fig. 5. (a) Output signal power of the booster as a function of the pump power at a fixed temperature for three different temperatures of 20 °C (black), 25 °C (red), and 40 °C (blue). (b) Output signal power as a function of the pump power at a fixed pump wavelength for two different pump wavelengths of 975 nm (black) and 980 nm (blue). The solid and open symbols represent measured data for the forward and backward pumping schemes of the booster, respectively. The curves in (a) are guides of the eyes, and the lines in (b) are linear fits of the measured data.

Figure 5(a) shows that the output signal power nonlinearly increased with the pump power for each operating temperature of the pump laser. For the forward pumping scheme at a fixed temperature of 25 °C, the output signal power approximately linearly increased with the pump power at a slope efficiency of about 22.8% for pump powers below 13.9 W. The slope efficiency significantly decreased and approached zero for pump powers between 16 and 19 W; consequently, the output signal power of the booster remained at around 3 W within this range of pump powers. Further increase in the pump power only slightly increased the output signal power. This efficiency suppression stemmed from the fact that the pump absorption coefficient of the gain fiber rapidly increased (from 2.6 to 3.8 m^{-1}) with the increase of the pump wavelength (from 971.3 to 973.8 nm) caused by the increasing drive current of the pump laser (from 6 to 8.5 A), as presented in Figs. 4(a) and 4(c). This effect resulted in strong absorption and depletion of the pump power in the beginning section of the gain fiber and insufficient pumping of the later section. Consequently, the increased pump power was not able to support the required level of population inversion throughout the whole length of the gain fiber to maintain the power conversion efficiency. Nevertheless, the output signal power started to increase with the pump power again when the pump power was increased above 19 W. This behavior resulted from the fact that, as presented in Figs. 4(a) and 4(c), the pump absorption coefficient remained at around 4 m^{-1} as the pump wavelength shifted from 974.3 to 975.3 nm when the drive current increased from 9 to 10 A at a fixed temperature of 25 °C. The pump absorption coefficient started to decrease with further increase in the drive current beyond 10 A while the operating temperature was fixed at 25 °C. As a result, the depletion of the pump power in the beginning section of the gain fiber was reduced and thus pumping of the later section of the gain fiber was increased. Accordingly, the increased pump power was again able to support population inversion throughout the gain fiber for an increased output signal power. Similar behaviors of the output signal power as a function of the pump power were observed at operating temperatures of 20 and 40 °C, as also presented in Fig. 5(a).

Compared with the forward pumping scheme, the backward pumping scheme provided a higher power conversion efficiency for all temperatures under investigation, as shown in Fig. 5(a). This is due to the fact that with backward pumping, the later section of the gain fiber was more sufficiently pumped than the beginning section; consequently, the signal saw increased population inversion as it propagated forward along the gain fiber, which allowed the signal to be continuously amplified until it reached the end of the gain fiber. This is quite opposite from the situation previously addressed for the forward pumping scheme, where the output signal power is determined mainly by the beginning section of the gain fiber, and

#239720 Received 24 Apr 2015; revised 13 Jun 2015; accepted 15 Jun 2015; published 6 Jul 2015

which therefore results in a lower power conversion efficiency than that for the backward pumping scheme at the same pump power. As also observed in Fig. 5(a), the difference in the output signal power between different operating temperatures is considerably smaller for the backward pumping scheme. This suggests that, for the backward pumping scheme, after propagating through the beginning section of the gain fiber, the signal was amplified to a level that it carried out large-signal amplification in the later section. Consequently, owing to the finite population inversion supported by each pump power level, the signal could only be amplified slightly as it propagated through the later section of the gain fiber. The longer the propagating distance in the gain fiber was, the slighter the amplification was in its later section. For the gain fiber used in this study, its length was so long that the output signal power was amplified to approach a level that the amplified output signal power is only slightly sensitive to the operating temperature of the pump laser.

Figure 5(b) demonstrates how the output signal power of the booster varies with the pump power by operating the pump laser at two fixed wavelengths, 975 and 980 nm, respectively, while its temperature varies with the drive current. For a fixed pump wavelength, the gain fiber has a fixed pump absorption coefficient no matter how the drive current of the pump laser varies. In this situation, the population inversion increases linearly with the drive current of the pump laser. As a result, for both pump wavelengths, when we fixed the pump wavelength by properly adjusting the temperature while varying the drive current, the output signal power increased linearly over the whole range of the pump power under study, which is very different from the result shown in Fig. 5(a). Because the pump absorption coefficients at 975 and 980 nm were 4 and 2.6 m^{-1}, respectively, the gain fiber should have absorbed more pump power and therefore should have provided more population inversion when it was pumped at 975 nm. Thus, it seems that a higher power conversion efficiency should be expected for the booster by operating the pump laser at 975 nm than operating it at 980 nm. However, as seen in Fig. 5(b), the power conversion efficiency for the pump wavelength at 975 nm was found to be smaller than that at 980 nm for either the forward or the backward pumping scheme. The discrepancy between the observed and the expected results can be explained by using the forward pumping scheme as an example. As previously addressed, in the forward pumping scheme, the signal saw decreased population inversion as it propagated along the gain fiber. Since the gain fiber under study was sufficiently long, over the range of the pump power levels under study, the later section of the gain fiber possessed deficient population inversion and thus turned out to absorb, not amplify, the signal. The extent of the decreased population inversion became more significant by operating the pump laser at 975 nm as the pump absorption coefficient is higher at this wavelength. This suggests that the later section of the gain fiber that absorbed the signal was longer by operating the pump laser at 975 nm, which led to stronger signal absorption and therefore a lower power conversion efficiency. These discussions indicate that, for a given length of the gain fiber, operating the pump laser at a wavelength that gives rise to a large pump absorption coefficient does not necessarily guarantee a high power conversion efficiency. Instead, a proper pump wavelength should be chosen for different operating conditions by adjusting the operating temperature of the pump laser in order to maximize the power conversion efficiency.

3.3.3 Maximization of power conversion efficiency

As demonstrated in the above, the power conversion efficiency of the booster depends on the pump power, the pump wavelength, the pumping scheme, and the length of the gain fiber. For a given booster, the pumping scheme and the gain fiber length are generally pre-determined and might not be easily changed. To achieve a specific power conversion efficiency at a specific pump power, therefore, a proper pump wavelength can be chosen by adjusting the pump laser temperature. By taking advantage of such capability in selecting the pump wavelength, we were able to vary the power conversion efficiency for each pump power level. Figure 6(a) shows the output signal power as a function of the pump power for the highest and lowest power conversion efficiencies of the booster. While the highest and lowest power conversion efficiencies respectively reached 22.2% and 15.4% for the forward

#239720 Received 24 Apr 2015; revised 13 Jun 2015; accepted 15 Jun 2015; published 6 Jul 2015

pumping scheme, higher conversion efficiencies of 31% and 26.7% were respectively achieved for the backward pumping scheme. For comparison, the power conversion efficiency obtained by operating the pump laser at the fixed wavelength of 975 nm, for either the forward or the backward pumping scheme, is also presented in Fig. 6(a). Interestingly, this power conversion efficiency is approximately that for the case of the lowest power conversion efficiency. This consistency again demonstrates that the later section of the gain fiber strongly absorbed, not amplified, the signal because of the long gain fiber used in this study. As shown in Fig. 4(b), because the largest pump absorption coefficient was found at the pump wavelength of 975 nm, the booster under study provided the lowest power conversion efficiency when the pump laser was operated at 975 nm. By using a shorter gain fiber of a properly optimized length for a given pump power to begin with so that no signal absorption occurs throughout the gain fiber, it is possible to take advantage of the largest pump absorption coefficient by operating the pump laser at 975 nm to achieve the highest possible power conversion efficiency of the booster.

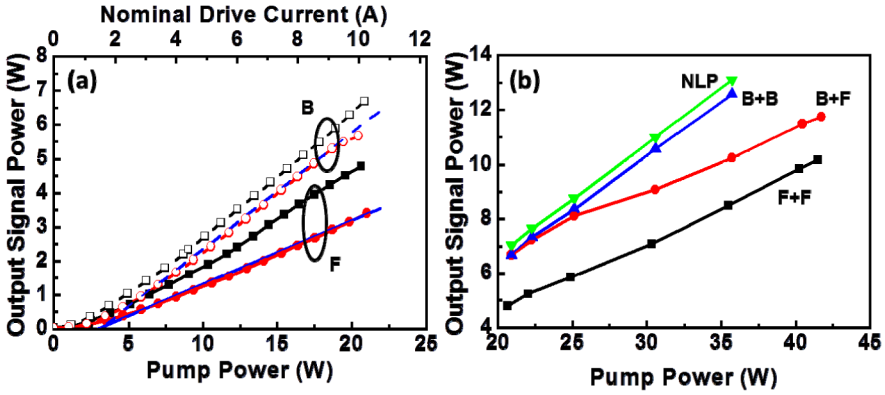

Fig. 6. (a) Output signal power of the booster as a function of the pump power for the highest (black curves and symbols) and lowest (red curves and symbols) power conversion efficiencies, respectively. The blue lines represent the output signal power by operating the pump laser at the fixed wavelength of 975 nm. (b) Output signal power of the booster as a function of the pump power for the highest power conversion efficiency by adding a second pump laser under three different pumping schemes. The letters "B" and "F" represent the backward pumping and forward pumping schemes, respectively. The green curve represents the highest power conversion efficiency of the booster for noise-like pulses (NLP) under dual-backward pumping.

To further enhance the output signal power of the given booster for the highest possible power conversion efficiency, a second pump laser was used to increase the total pump power. The result is demonstrated in Fig. 6(b). Three different pumping schemes were considered, namely dual-forward pumping, bidirectional pumping, and dual-backward pumping. For each operating condition, the two pump lasers was successively applied and temperature-adjusted to maximize the output signal power. Note that, for the bidirectional pumping scheme, the backward pumping was applied first and the forward pumping next. As demonstrated, the dual-backward pumping scheme provided the highest power conversion efficiency of 34.7%. As a result, an output signal power of 12.6 W at a total pump power of 35.7 W was obtained. Since the maximum levels of the signal power and the pump power both happened at the signal output end of the gain fiber for the dual-backward pumping scheme, there existed considerable heat accumulation at this location, which could damage the fused interface between the gain fiber and the signal–pump power combiner. This effect therefore limited our ability to increase the total pump power beyond 35.7 W for an even higher output signal power. A fused interface that has an improved ability to handle higher optical power should enable further enhancement of the output signal power. For the other two pumping schemes, we were able to increase the total pump power beyond 35.7 W because the heat was

#239720 Received 24 Apr 2015; revised 13 Jun 2015; accepted 15 Jun 2015; published 6 Jul 2015

distributed to the two ends of the gain fiber. The maximum output signal power obtained for the bidirectional and dual-forward pumping schemes were 11.7 and 10.2 W, respectively, at a total pump power of around 41.6 W, leading to power conversion efficiencies of 27.6% and 24%, respectively.

3.4 Amplification of noise-like pulses with booster

The understanding obtained above on the output behavior of the booster by using continuous-wave optical fields serves as an operating guidance for pulse amplification. The pre-amplified noise-like pulses at a repetition rate of 15.5 MHz with an average power of 0.21 W presented in Section 3.2 was sent into the booster under dual-backward pumping, the result of which is presented as the green curve in Fig. 6(b). Thus, an average power of 13.1 W and a pulse energy of 0.85 μJ for the output signal were achieved at a pump power of 35.7 W, which, to the best of our knowledge, are the highest achieved levels for noise-like pulses in the 1.56-μm wavelength region. A gain of 18 dB and a power conversion efficiency of 36.1% in the booster were reached. As presented in Fig. 7(a), the 3-dB spectral bandwidth of the amplified noise-like pulses at the output of the booster slightly increased over that of the input pulses to 22 nm. Compared with the spectrum of the pulses at the output of the pre-amplifier, spectral broadening after the booster was seen in the spectral regions below 1515 nm and above 1620 nm, respectively, where the wavelengths occupied a low proportion of the whole spectral power. Thus, the spectral broadening effect was not significant in the booster. This favorable result could be attributed to the utilization of the large-mode-area fiber to reduce intensity, thus suppressing the nonlinear optical effects, in the booster at the high power level of our system. Note that a signal with an over-broadening spectrum might lead to a low gain efficiency in an amplifier, which should been avoided particularly for conducting high-power noise-like pulse amplification.

It is worth mentioning that the amplification characteristics of the booster, such as the power conversion efficiency shown in Figs. 5 and 6, for both continuous-wave and noise-like pulse inputs were observed to be closely similar. This is due to the facts explained below. First, the repetition rate of the noise-like pulses in our study is 15.5 MHz, which is much higher than the decay rate (on the order of 100 s^{-1}) of the excited erbium ions of the booster gain fiber. This makes the noise-like pulses more like continuous-wave signals than pulses for the booster. Second, the gain medium of the booster used in our study is a 25-μm large-mode-area fiber, which can withstand pulses of much higher peak power before significant fiber nonlinearity is induced, as compared with an 8-μm standard fiber. The absence of significant nonlinear effect was verified by a comparison between the measured optical spectra presented in Figs. 3(a) and 7(a), which shows that the 3-dB spectral width of the noise-like pulses only slightly differed by 1 nm after significant power amplification from 0.21 W to 13.1 W by the booster. Third, the gain bandwidth of the gain fiber is broader than the spectral width of the noise-like pulses.

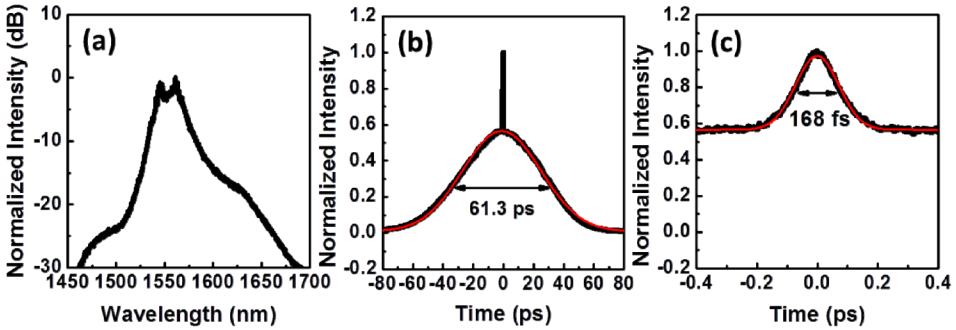

Fig. 7. (a) Output optical spectrum, (b) autocorrelation trace, and (c) magnified autocorrelation trace of noise-like pulses from the booster. Red curves in (b) and (c) are the Gaussian fittings of the pedestal and the peak, respectively.

#239720 Received 24 Apr 2015; revised 13 Jun 2015; accepted 15 Jun 2015; published 6 Jul 2015

Figures 7(b) and 7(c) show the autocorrelation trace of the noise-like pulse train after amplification by the booster. The observed pedestal-to-peak intensity ratio was only slightly higher than 0.5, which is a key feature of the noise-like pulses. In addition, the peak width further shortened to 168 fs, and the pedestal width slightly lengthened to 61.3 ps. Therefore, the characteristics of the noise-like pulse train were kept approximately the same before and after the amplification by the booster.

4. Conclusion

We developed a high-power noise-like pulse laser system at 1.56 μm comprising of a seed fiber ring oscillator and a two-stage fiber amplifier. The average power of the seed pulse train was increased to a medium power level through a pre-amplifier based on an erbium-doped gain fiber, and it was then boosted to a high-power level by a booster based on an erbium/ytterbium-codoped gain fiber. The power conversion efficiency of the booster was investigated by adjusting the wavelength of the diode laser pumping the fiber amplifier. The pump wavelength, which determines the pump absorption and therefore the power conversion efficiency of a gain fiber, was properly adjusted through changing the temperature of the pump diode laser under various operating conditions to maximize the power conversion efficiency. Three different dual-pumping schemes were also investigated while applying this efficiency-enhancement procedure. This approach was proved and supplied as a guideline for amplifying the noise-like pulses to a high power level. By applying the dual-backward pumping scheme to the booster, the average power of the noise-like pulse train was amplified considerably from an input of 0.21 W to an output of 13.1 W at a total pump power of 35.7 W. This process resulted in a power conversion efficiency of 36.1% and a pulse energy of 0.85 μJ. A net gain as high as 30 dB was obtained. With peak and pedestal widths of 168 fs and 61.3 ps, respectively, for the amplified pulses, the pedestal-to-peak intensity ratio of the autocorrelation trace remained at the value of 0.5 required for truly noise-like pulses. Thus, the characteristics of the noise-like pulse train were properly maintained after propagating through the two cascaded amplifiers.

Acknowledgments

S.K. Hwang's work is supported by the Ministry of Science and Technology of Taiwan under Contract MOST103-2112-M-006-013-MY3.

#239720 Received 24 Apr 2015; revised 13 Jun 2015; accepted 15 Jun 2015; published 6 Jul 2015